SUPPORTING INFORMATION

Nanotopographic Regulation of Human Mesenchymal Stem Cell Osteogenesis

Weiyi Qian[1], Lanqi Gong[1], Xin Cui[1], Zijing Zhang[1], Apratim Bajpai[1], Chao Liu[1,2], Alesha B. Castillo[1,2], Jeremy C. M. Teo[3], and Weiqiang Chen[1*]

[1]Department of Mechanical and Aerospace Engineering, New York University, New York, NY 11201, USA; [2]Department of Orthopaedic Surgery, School of Medicine, New York University, New York, NY 10003, USA; [3]Department of Biomedical Engineering, Khalifa University, P.O. Box 127788, Abu Dhabi, 127788, UAE.

[*]Correspondence should be addressed to W. Chen (email: wchen@nyu.edu)

Supporting Information:

Supporting Figures & Tables and Captions

Figure S1

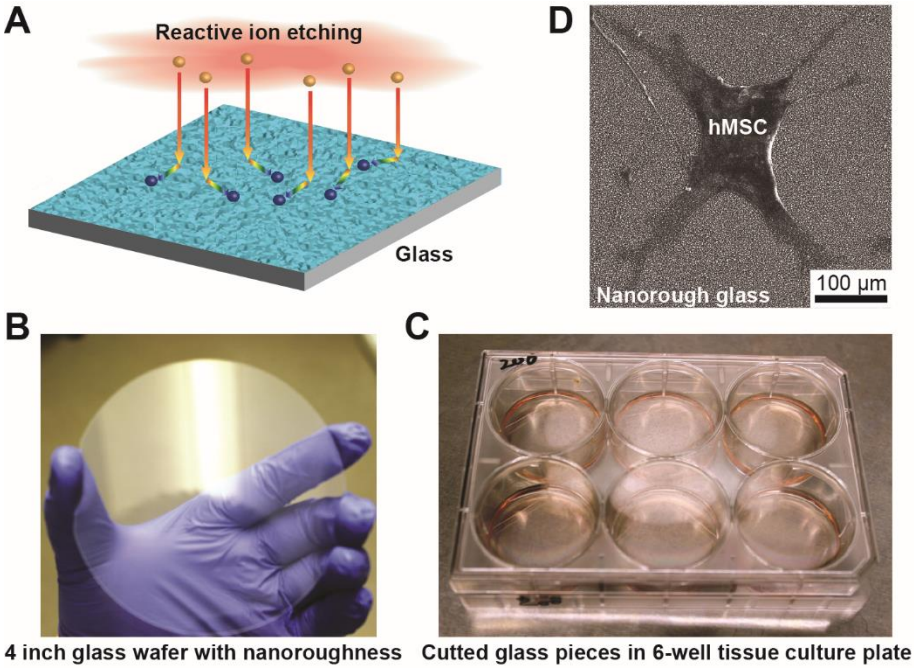

Figure S1. Nanoengineered nanotopographic surfaces. (**A**) Schematic of nanotopography generated by RIE on glass surfaces. (**B**&**C**) Photograph showing a 4-inch glass wafer with nanotopographic features (B) before cut and placed into tissue culture dishes (C). (**D**) Representative SEM image showing hMSC plated on nanorough glass surface.

Figure S2

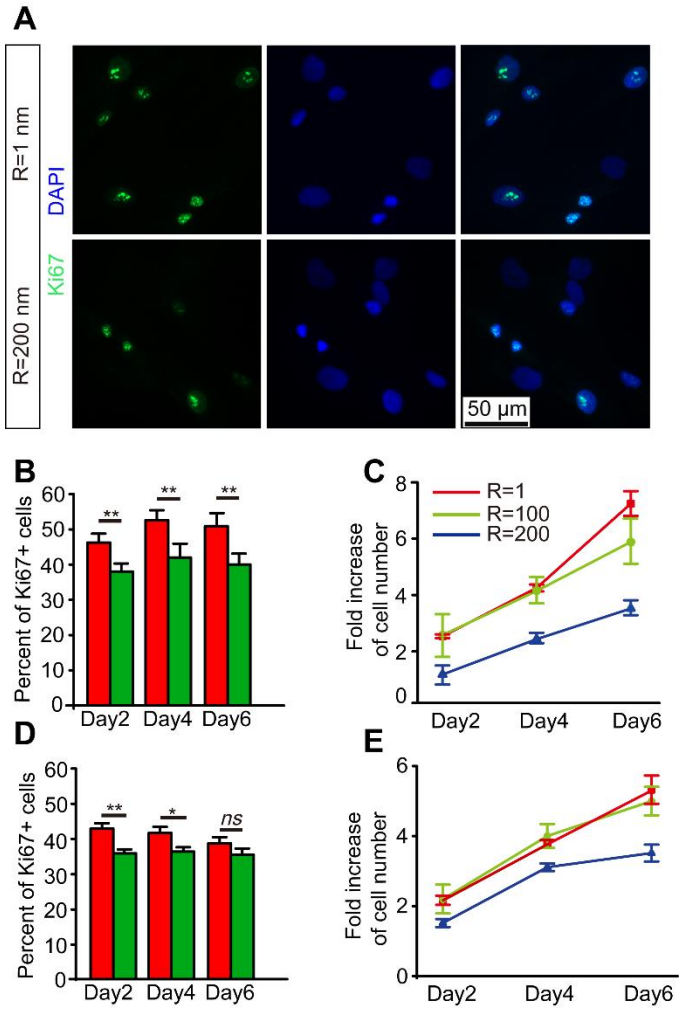

Figure S2. Proliferation of hMSCs on different nanotopographies with cell growth and differentiation media. **(A)** Representative immunofluorescence images of Ki67 expression (green) and nuclear (DAPI; blue) in hMSCs on smooth (R_q = 100 nm) and nanorough (Rq = 200 nm) surface in culture medium. (**B**) Bar plot showing percentages of Ki67+ hMSCs on smooth (R_q = 1 nm) and nanorough (R_q = 200 nm) surface at different days of culture with cell growth meida. (**C**) Fold increase of cell number based on DAPI quantification over 6 days of culture on smooth (R_q = 1 nm) and nanorough (R_q = 200 nm) surface with cell growth media. (**D**) Bar plot showing percentages of Ki67+ hMSCs on smooth (R_q = 1 nm) and nanorough (R_q = 200 nm) surface at different days of culture with osteogenic differentiation media. (**E**) Fold increase of cell number based on DAPI quantification over 6 days of culture on smooth (R_q = 1 nm) and nanorough (R_q = 200 nm) surface with osteogenic differentiation media.

Figure S3

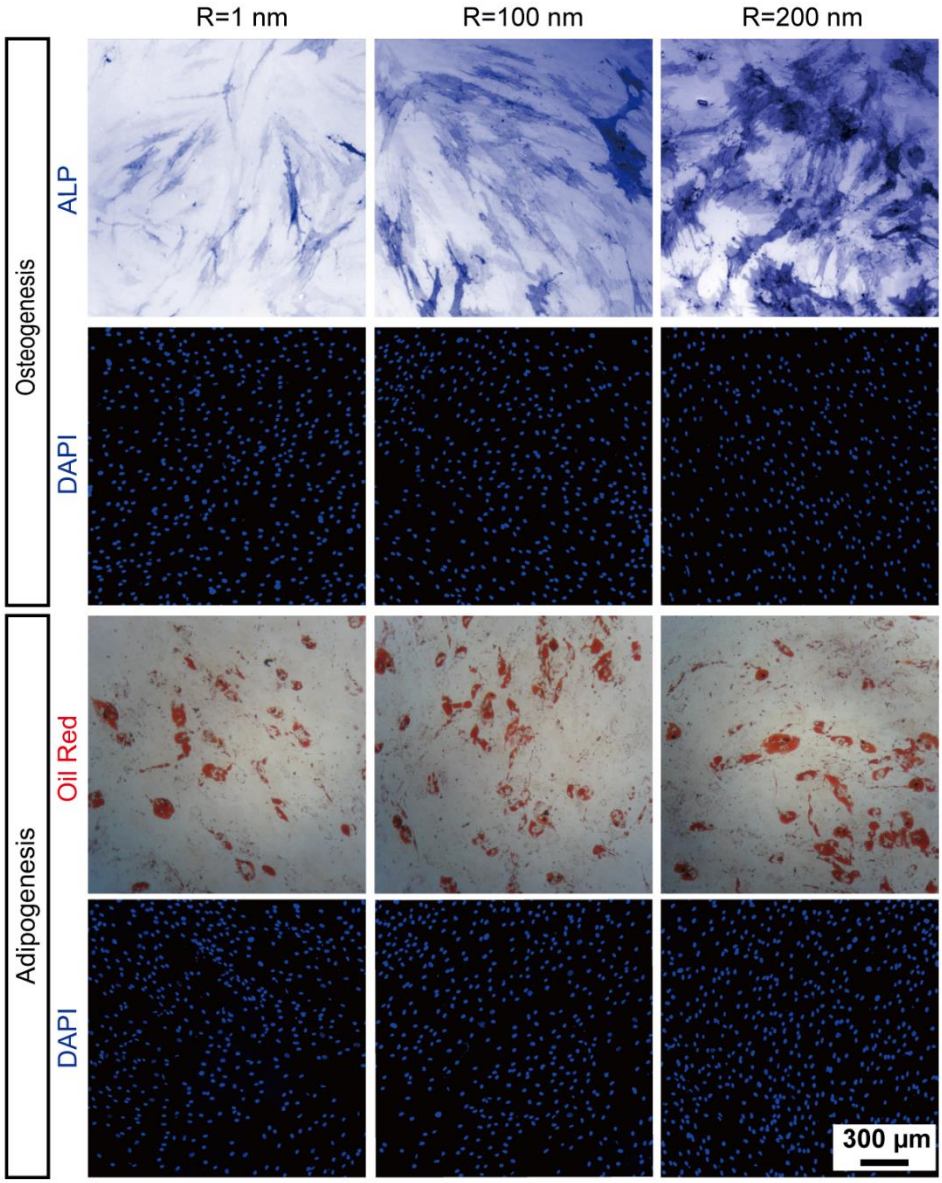

Figure S3. Representative ALP and oil red staining images showing hMSC osteogenesis and adipogenesis for 7 and 14 days respectively in osteogenic and adipogenic differentiation medium on smooth (R_q = 1 nm) and nanorough (R_q = 100, 200 nm) glass substrates as indicated.

Figure S4

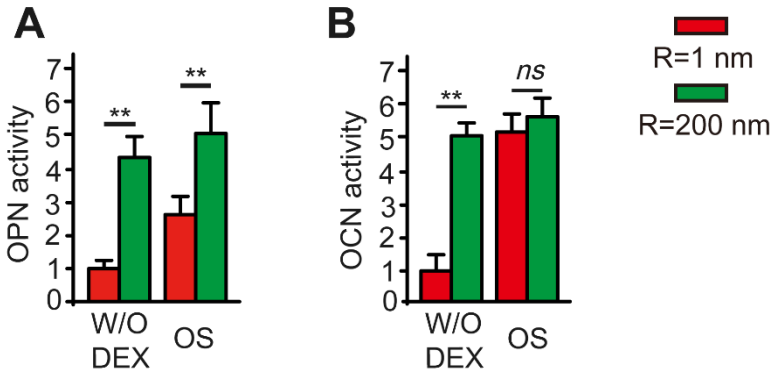

Figure S4. Quantification of OPN (A) and OCN (B) activities based on the fluorescent intensity of immunofluorescent stained images after 21 days of differentiation in conditioned osteogenic differentiation media on smooth (R_q = 1 nm) and nanorough (R_q = 200 nm) glass surfaces as indicated.

Figure S5

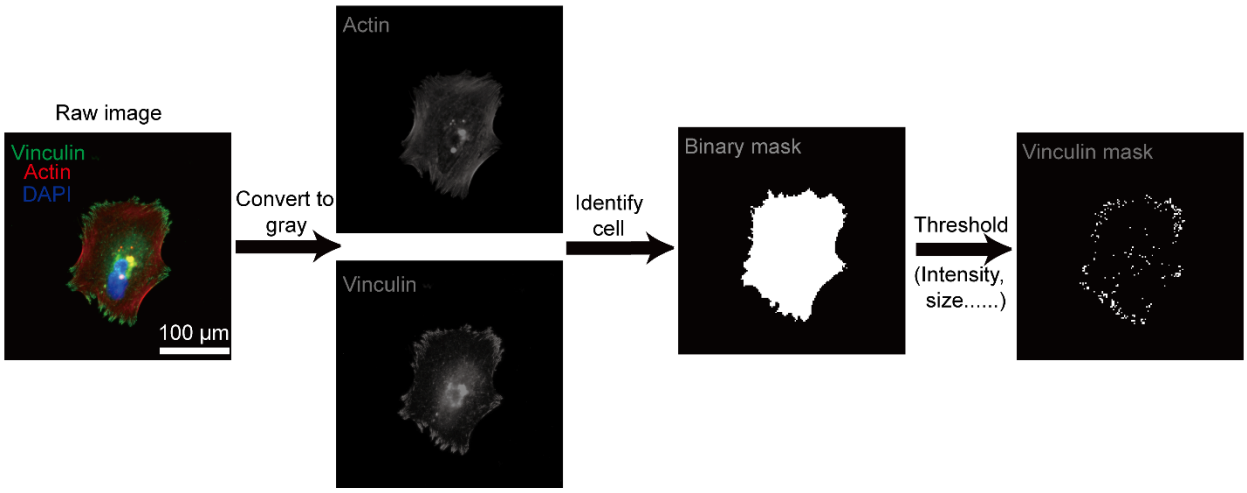

Figure S5. Quantification of FAs and β_1 integrin subunits. The quantification of FAs and β_1 integrin subunits was achieved by imaging processing of immunofluorescent stained images using customized Matlab code carrying out above process. Cell actin was used to identify cell area, vinculin and β_1 integrin were then quantified by applying binary mask thresholds, respectively.

Figure S6

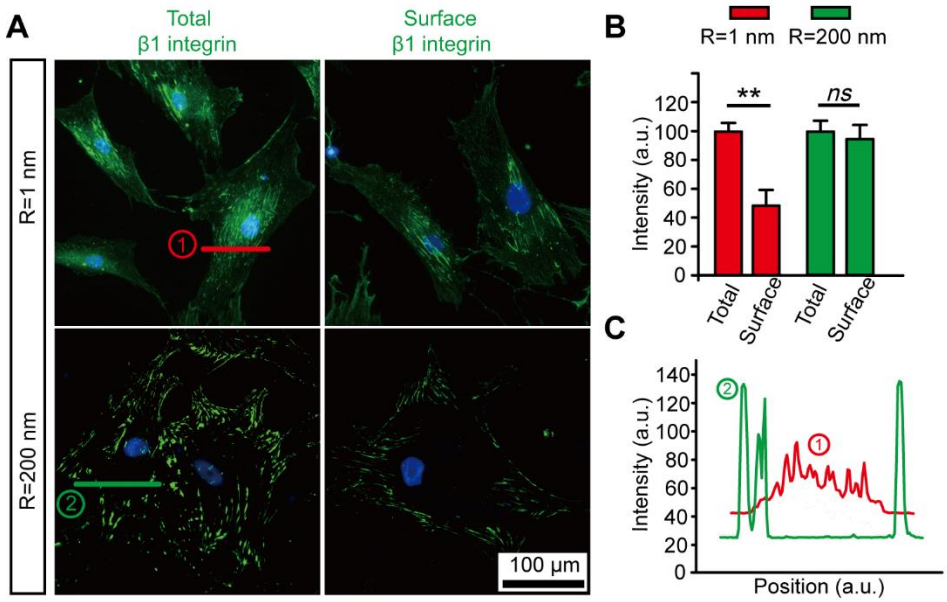

Figure S6. Quantification of β_1 integrin activity in hMSCs. (**A**) Immunofluorescence images and (**B**) Quantification of total and surface β_1 integrin in undifferentiated hMSCs on smooth (R_q = 1 nm) and nanorough (R_q = 200 nm) glass substrates after 24 hr of culture. (**C**) Total β_1 integrin distribution across single hMSCs cultured on smooth (R_q = 1 nm; red line) and nanorough (R_q = 200 nm; blue line) glass substrates.

Figure S7

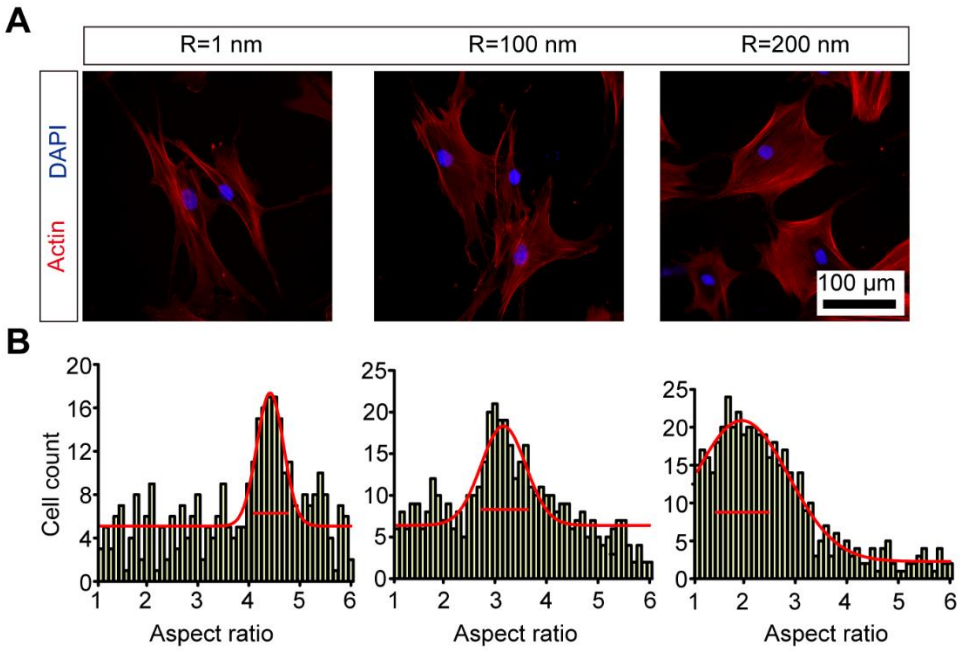

Figure S7. Quantitative analysis of cell morphological aspect ratio. (**A**) Representative actin immunofluorescence images showing cell morphology and (**B**) distributions of cell morphological aspect ratio of hMSCs after 24 hours of culture on smooth (R_q = 1 nm) and nanorough (R_q = 100, 200 nm) surfaces.

Figure S8.

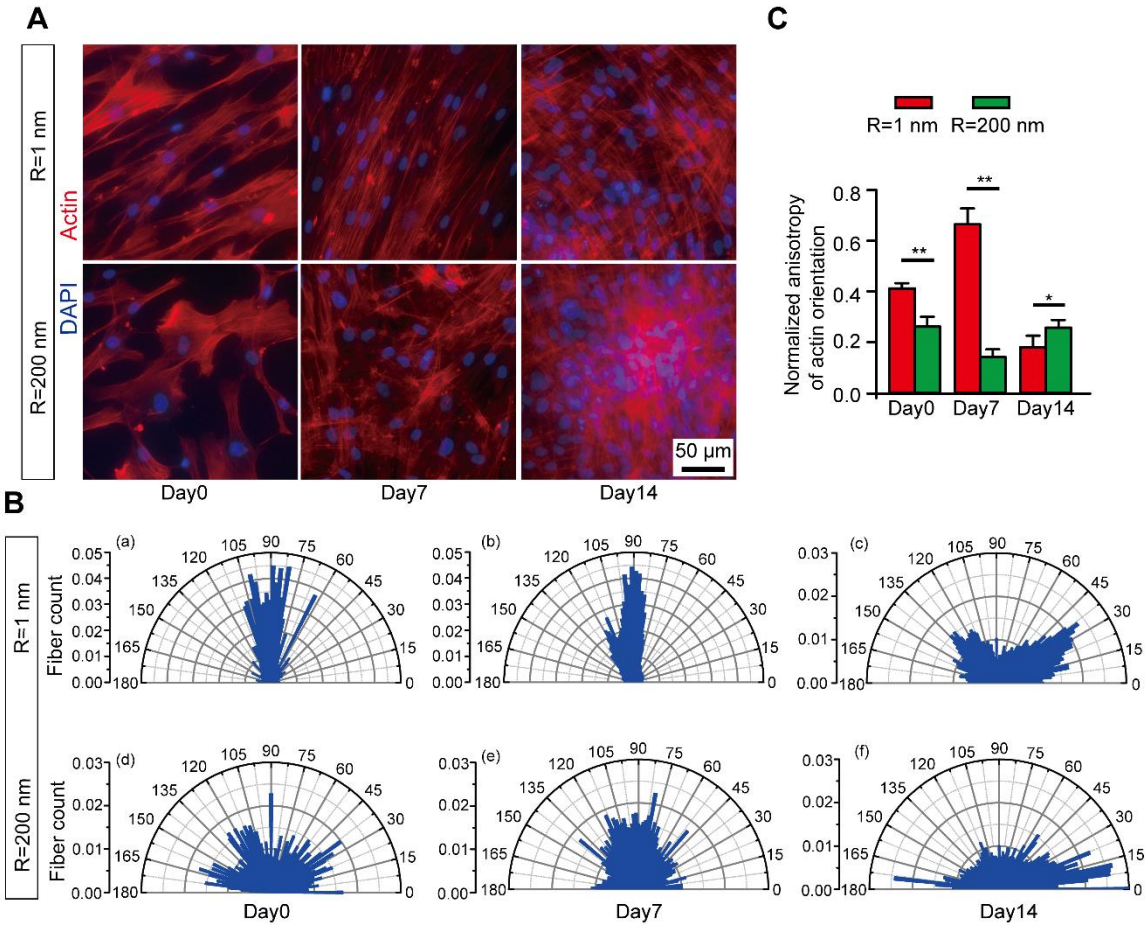

Figure S8. Nanoroughness-induced spontaneous collective actin CSK remodeling in hMSC colony during early osteogenic differentiation stage. (**A**) Representative immunofluorescence images of collective actin orientations in hMSC colony during the early days of osteogenic differentiation on smooth (R_q = 1 nm) and nanorough (R_q = 200 nm) surface as indicated. (**B**) Representative rose plots of the actin angles in hMSCs with respective to the actin immunofluorescence images in (A). (**C**) Quantitative analysis of hMSC actin anisotropy at different days of osteogenic differentiation on smooth (R_q = 1 nm) and nanorough (R_q = 200 nm) surfaces as indicated.

Figure S9.

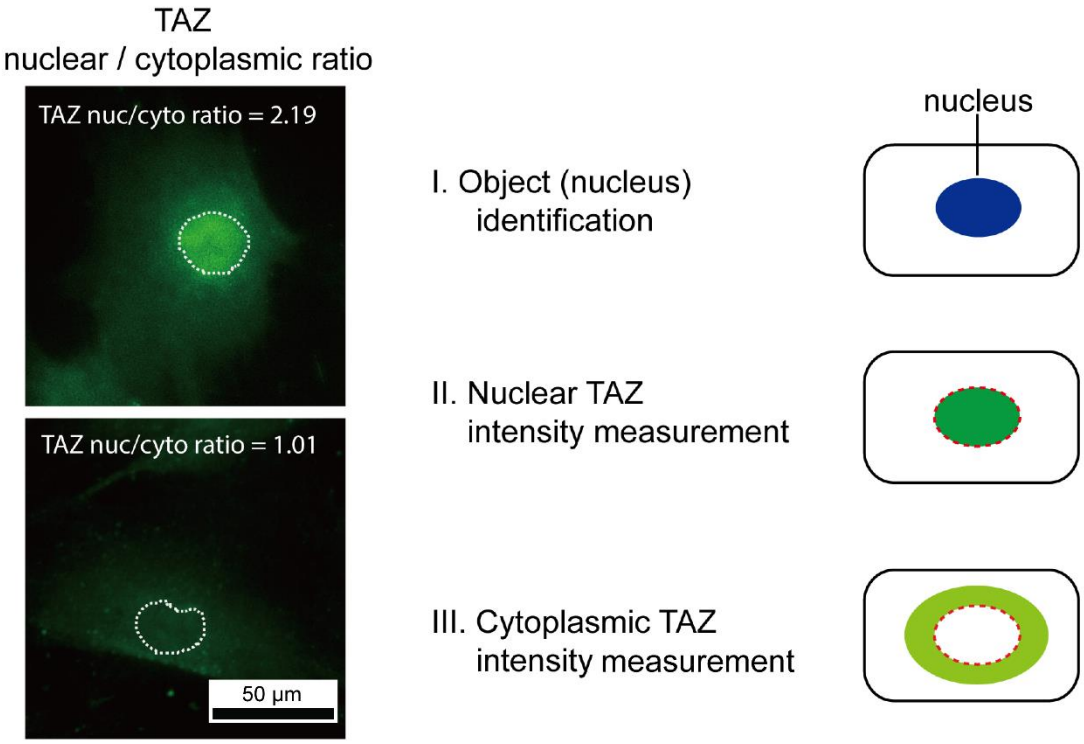

Figure S9. Quantification of TAZ nuclear/cytoplasmic ratio. The TAZ nuclear/cytoplasmic ratio in each cell was determined by the nuclear/cytoplasmic ratio of TAZ mean fluorescence intensities (nuc/cyto ratio).

Figure S10.

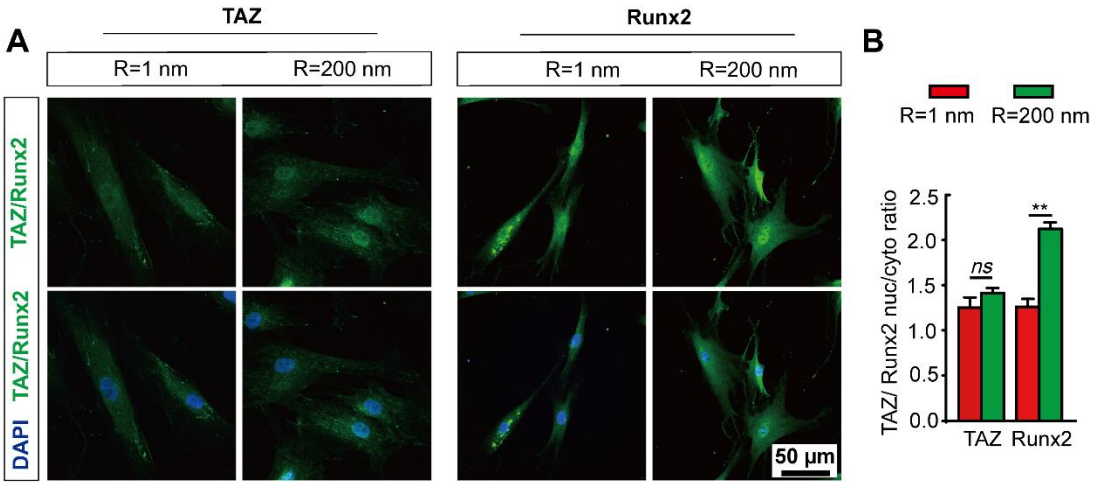

Figure S10. Nucleocytoplasmic shuttling of TAZ and Runx2 in hMSCs. (A) Representative immunofluorescence images, and (**B**) Bar plot showing nanoroughness-dependent subcellular localization of TAZ and Runx2 at day 0 (R_q = 1 nm) and nanorough (R_q = 200 nm) glass surfaces as indicated.

Figure S11.

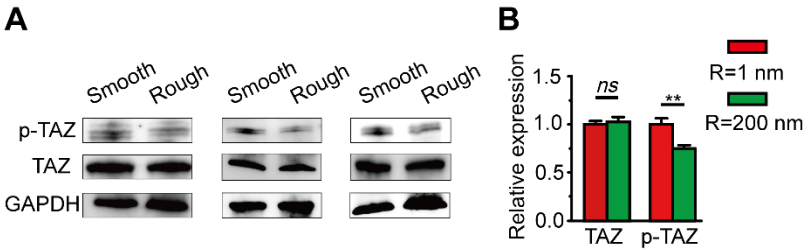

Figure S11. Three replicates of western results and statistic results for TAZ phosphorylation on on smooth (R_q = 1 nm) and nanorough (R_q = 200 nm) glass surfaces as indicated.

Figure S12.

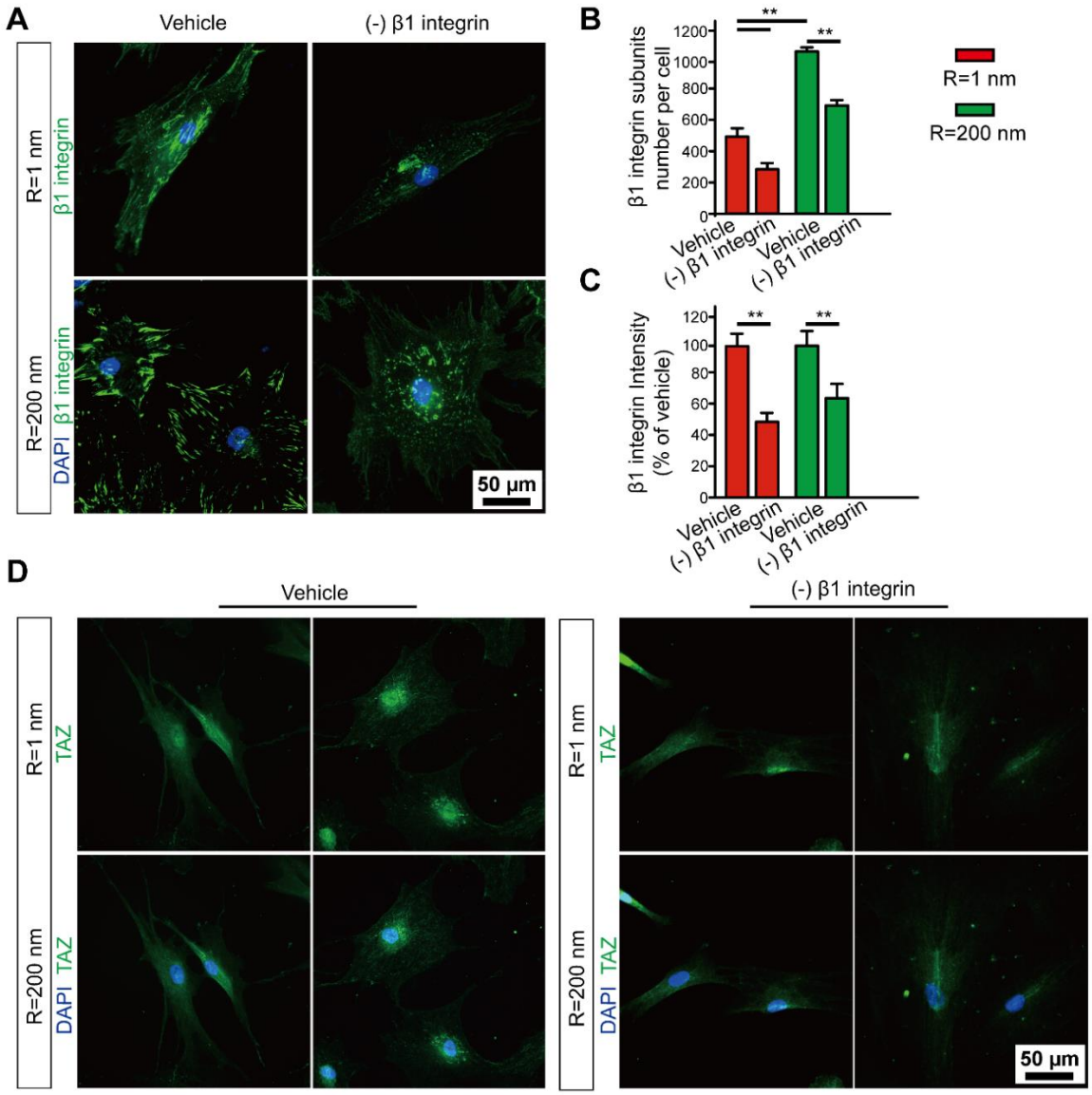

Figure S12. Inhibition of β_1 integrin and corresponding regulatory effect on nucleocytoplasmic shuttling of TAZ in hMSCs. (**A**) Representative immunofluorescence images showing β_1 integrin and (**B-C**) quantification of β_1 integrin subunit number (B) and intensity (C) in undifferentiated hMSCs on smooth (R_q = 1 nm) and nanorough (R_q = 200 nm) glass substrates treated with or without (vehicle) β_1 integrin inhibitor for 24 hr. (**D**) Representative immunofluorescence images of TAZ and nucleus DAPI for hMSCs on smooth (R_q = 1 nm) and nanorough (R_q = 200 nm) glass substrates treated with or without (vehicle) β_1 integrin inhibitor for 24 hr.

Figure S13.

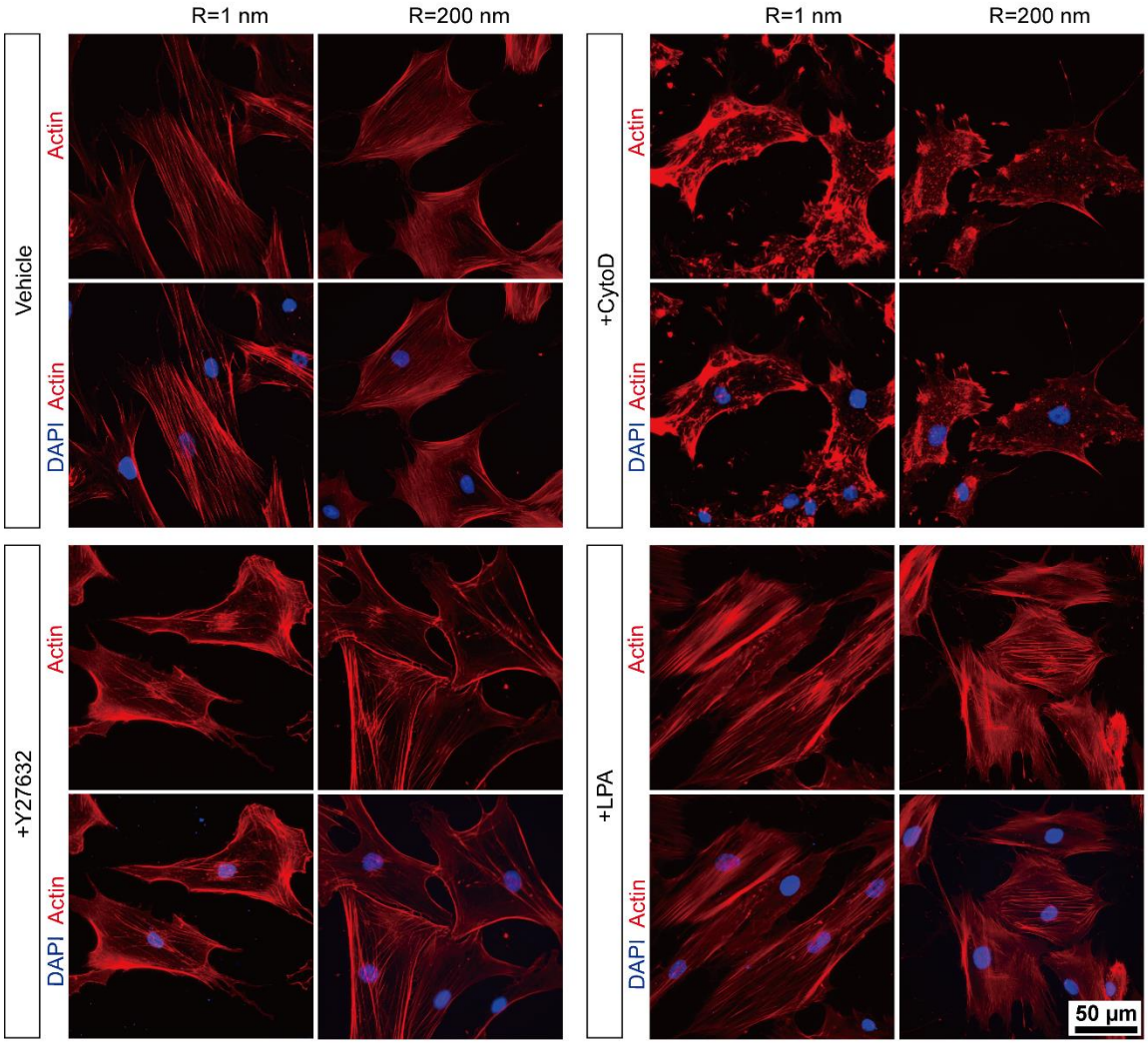

Figure S13. Actin CSK structures of hMSCs under CSK disturbing drug treatments. Immunofluorescence images showing actin structures of hMSCs on smooth (R_q = 1 nm) and nanorough (R_q = 200 nm) glass substrates after 24 h treatment in osteogenic induction medium supplemented with DMSO (vehicle control), ROCK inhibitor Y27632, actin polymerization inhibitor cytochalasin D (CytoD), and RhoA activator lysophosphatidic acid (LPA), as indicated.

Figure S14.

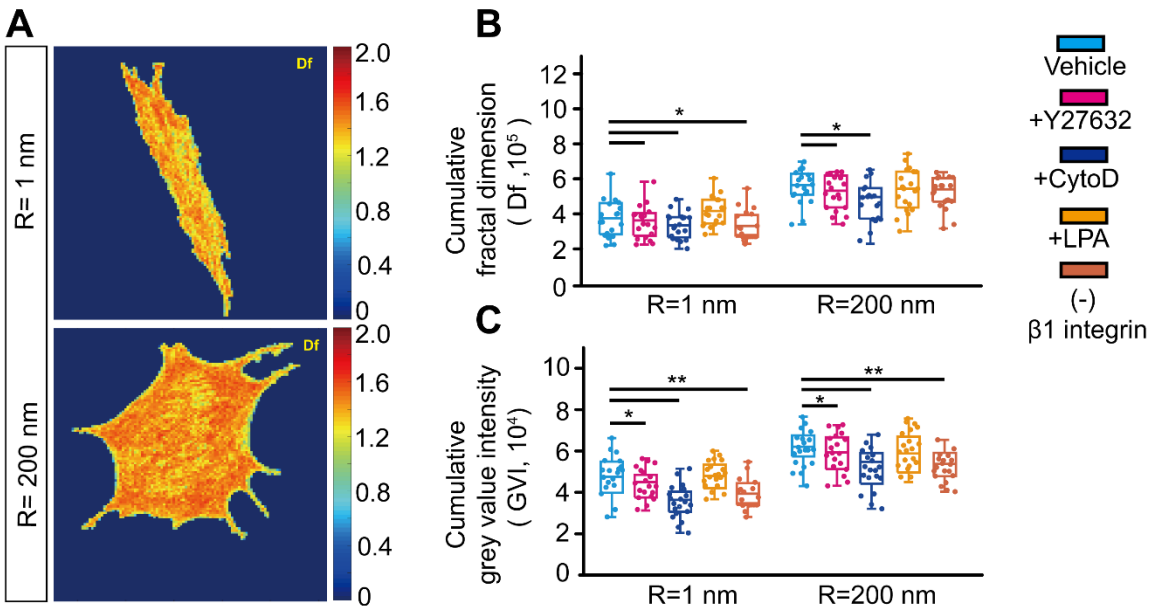

Figure S14. Characterization of subcellular actin CSK structure and intensity under drug treatment. (**A**) Representative fractal dimension (D_f) heat map of hMSCs on smooth (R_q = 1 nm; top) and nanorough (R_q = 200 nm; bottom) glass substrates. (**B-C**) Quantification of D_f (B) and gray value intensity (C) of hMSCs cultured for 24 hours in osteogenic induction medium supplemented with DMSO (vehicle control), ROCK inhibitor Y27632, actin polymerization inhibitor cytochalasin D (CytoD), and RhoA activator lysophosphatidic acid (LPA), as indicated.

Figure S15.

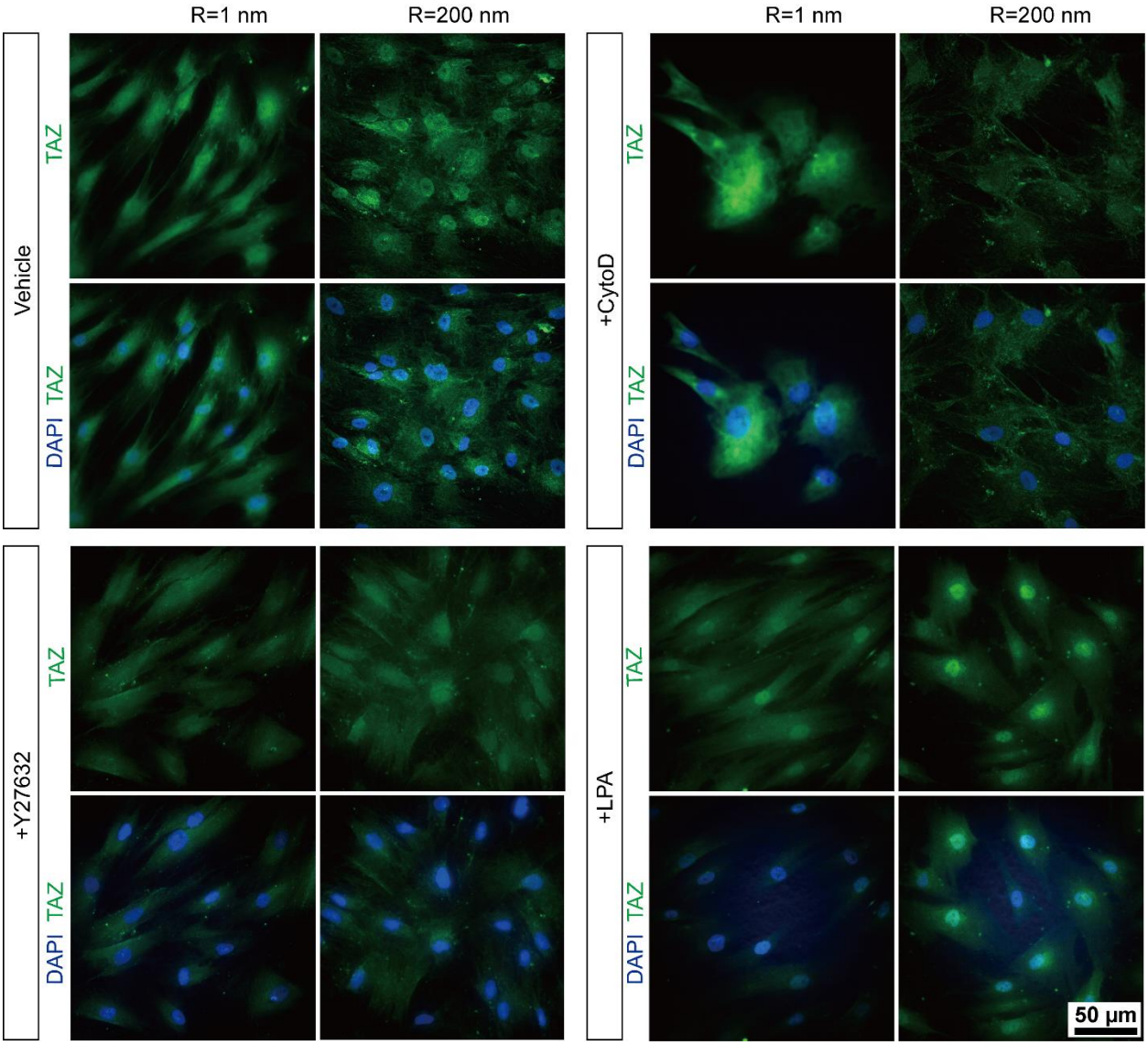

Figure S15. Regulation of nucleocytoplasmic shuttling of TAZ in hMSCs by actomyosin contractility and actin cytoskeleton (CSK) integrity. Immunofluorescence images show subcellular localization of TAZ in hMSCs on smooth (R_q = 1 nm) and nanorough (R_q = 200 nm) glass substrates cultured for 24 hours in osteogenic induction medium supplemented with DMSO (vehicle control), ROCK inhibitor Y27632, actin polymerization inhibitor cytochalasin D (CytoD), and RhoA activator lysophosphatidic acid (LPA), as indicated.

Figure S16.

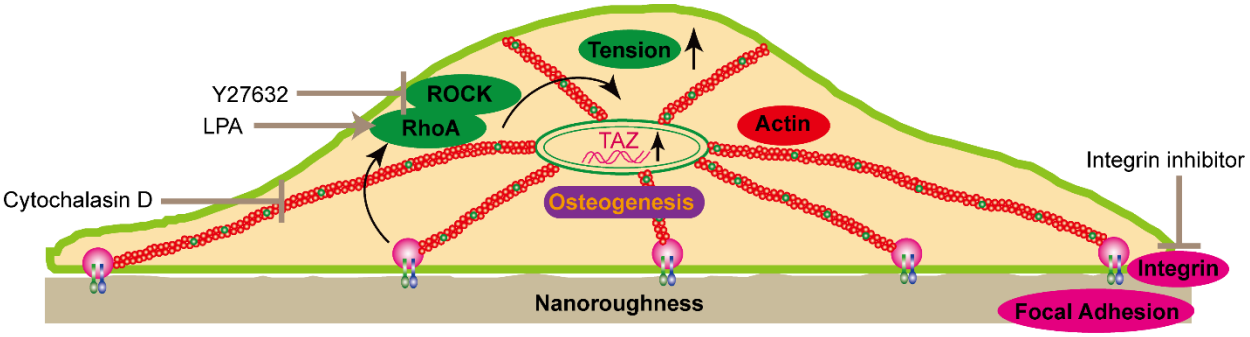

Figure S16. Nanoroughness-induced hMSC osteogenesis is activated through triggering integrin-CSK-nuclear TAZ signaling.

Table S1. List of antibodies used in immunofluorescence and western blotting.

Protein	Vendor	Catalog number	Dilution
p-Smad1,5,8	Millipore	AB3848-I	1:500 (WB)
Smad1,5,8	Novusbio	nb100-56656	1:500 (WB)
p-FAK	Abcam	ab39967	1:500 (WB), 1:100 (IF)
GAPDH	Santa-Cruz Biotechnology	sc-25778	1:1000 (WB)
TAZ	Santa-Cruz Biotechnology	sc-48805	1:500 (WB), 1:100 (IF)
p-TAZ	Cell Signaling	75275	1:1000 (WB)
Ki-67	Biolegend	350501	1:100 (IF)
OPN	Santa-Cruz Biotechnology	sc-20788	1:100 (IF)
OCN	Santa-Cruz Biotechnology	sc-376835	1:100 (IF)
Total β_1 integrin	Millipore	MAB2247-I	1:200 (IF)
Activated β_1 integrin	Millipore	MAB2079Z	1:200 (IF)
Vinculin	Sigma	V9131	1:100 (IF)
Runx2	Santa-Cruz Biotechnology	sc-390351	1:100 (IF)